LA-2703

C.4

LOS ALAMOS SCIENTIFIC LABORATORY
OF THE UNIVERSITY OF CALIFORNIA o LOS ALAMOS NEW MEXICO

THE HYDRODYNAMIC HOT SPOT AND SHOCK INITIATION OF HOMOGENEOUS EXPLOSIVES

Printed in USA Price $ 1.00. Available from the

Office of Technical Services
U. S. Department of Commerce
Washington 25, D. C.

LA-2703
PHYSICS
TID-4500 (17th Ed.)

LOS ALAMOS SCIENTIFIC LABORATORY
OF THE UNIVERSITY OF CALIFORNIA LOS ALAMOS NEW MEXICO

REPORT WRITTEN: March 23, 1962

REPORT DISTRIBUTED: July 18, 1962

THE HYDRODYNAMIC HOT SPOT AND SHOCK INITIATION OF HOMOGENEOUS EXPLOSIVES

by

Charles L. Mader

Contract W-7405-ENG. 36 with the U. S. Atomic Energy Commission

ABSTRACT

The shock initiation of nitromethane, liquid TNT, and single-crystal PETN has been computed using one-dimensional numerical reactive hydrodynamics and realistic equations of state. The computed pressures and velocities as functions of time agree with the experimental values to within the probable experimental error.

The initiation of shocked nitromethane by spherical hydrodynamic hot spots was investigated. When a hydrodynamic hot spot has decomposed, it sends a shock wave into the undetonated explosive and heats it. What occurs thereafter depends upon the initial strength of the shock wave and how well it is supported from the rear. Whether the explosion of the hot spot propagates to the rest of the fluid or not depends primarily on the initial size of the hot spot.

ACKNOWLEDGMENT

The author gratefully acknowledges the assistance and contributions of Francis Harlow of LASL Group T-3 and William C. Davis, Wildon Fickett, John Zinn, Charles Forest, and Louis C. Smith of the LASL GMX Division.

CONTENTS

		Page
ABSTRACT		3
ACKNOWLEDGMENT		3
I.	INTRODUCTION	7
II.	THE COMPUTATIONAL METHOD	9
III.	RESULTS OF THE SHOCK INITIATION CALCULATIONS	10
IV.	HYDRODYNAMIC HOT SPOT CALCULATIONS	13
	A. Temperature Hot Spots	14
	B. Pressure Hot Spots	22
	C. Hydrodynamic Hot Spot Summary	25
V.	CONCLUSIONS	25
APPENDIX A	THE HYDRODYNAMIC EQUATIONS	27
APPENDIX B	THE EQUATION OF STATE	34
LITERATURE CITED		42

TABLES

Table I.	Shock Initiation of Nitromethane, Liquid TNT, and PETN	12
Table BI.	Equation of State and Rate Parameters	36
Table BII.	BKW Computed C-J Parameters	37

ILLUSTRATIONS

		Page
Fig. 1	Shock Initiation of Nitromethane by a 92 kbar Shock	11
Fig. 2	Development of a Detonation in Shocked Nitromethane from a 0.292 cm Radius Spherical Temperature Hot Spot	15
Fig. 3	Development of a Detonation in Shocked Nitromethane from a 0.06 cm Radius Spherical Temperature Hot Spot	17
Fig. 4	Failure of a 0.0292 cm Radius Spherical Temperature Hot Spot to Develop into a Detonation in Shocked Nitromethane	19
Fig. 5	Failure of a 0.27 cm Radius Spherical Temperature Hot Spot to Develop into a Detonation in Unshocked Nitromethane	20
Fig. 6	Development of a Detonation in Shocked Nitromethane from a 0.03 cm Radius Spherical Pressure Hot Spot	23
Fig. 7	Failure of a 0.0175 cm Radius Spherical Pressure Hot Spot to Develop into a Detonation in Shocked Nitromethane	24

I. INTRODUCTION

The shock initiation of homogeneous explosives has been extensively investigated by Campbell, Davis, and Travis[1]. They observed that the detonation of the heated, compressed explosive begins at the interface, where the explosive has been hot the longest, after an induction time which is a decreasing function of the shock strength. The detonation proceeds through the compressed explosive at a velocity greater than the steady state velocity in uncompressed explosive, overtaking the initial shock and overdriving the detonation in the unshocked explosive.

The reactive hydrodynamics of shock initiation has been investigated by Hubbard and Johnson[2] and by Enig[3]. The results of their calculations qualitatively resembled the experimental observations of Campbell, Davis, and Travis[1]. However, quantitative agreement between the experimental and computed pressures and velocities as a function of time was not obtained because of the unrealistic equations of state. We have attempted to use the best numerical reactive hydrodynamics and as realistic equations of state as are available to determine if we could obtain quantitative agreement with the experimental observations.

Since any realistic equation of state is somewhat involved, it was necessary to use electronic computers and considerable amounts of machine time to obtain the desired quantitative agreement.

Having found this comparison reasonably successful, we investigated the hydrodynamics of hot spots. Experimentally[1] it has been observed that

0.05 to 0.02 cm radius bubbles in shocked nitromethane caused reacting hot spots in the liquid nitromethane that either exploded and propagated or failed to propagate in times of the order of 0.1 μsec. Evans, Harlow, and Meixner[4] have computed that the interaction of a shock with a bubble in nitromethane produces hot spots in the liquid nitromethane of the same order of magnitude in size as the original bubbles. Thus, reacting hot spots of the order of 0.05 to 0.01 cm radius should explode and propagate or fail to propagate in times of the order of 0.1 μsec.

Zinn[5] has shown that the thermal conductivity model hot spot does not result in propagation of an explosion. He has also shown that chemical reaction must be well under way by the end of the interval $0.04\ (R^2)/k$, or cooling by heat conduction prevents the hot spot from exploding. The thermal diffusivity k, is $\lambda/\rho c$, where λ is heat conductivity, ρ is density, and c is heat capacity. A reasonable value for k for nitromethane is 0.001. To fail in 0.1 μsec, a thermal conductivity hot spot must have a radius smaller than 5×10^{-5} cm. Quenching of a 0.01 cm radius hot spot takes 4000 μsec. It is immediately apparent that the thermal conductivity hot spot is unsatisfactory as a model to explain the experimental observations[1] and computed shock interaction results[4] for hot spots in shocked nitromethane. A new model is required, and we propose that the hydrodynamic hot spot model is at least qualitatively satisfactory.

The introduction of kinetics into a numerical hydrodynamic calculation raises the question of how satisfactorily the calculation reproduces the interaction of kinetics and hydrodynamics. Presently, it is necessary to perform numerical experiments and compare the results with known steady state results. For example, comparison of gamma-law Taylor waves and matched pressures across boundaries with numerical results indicate that the kinetics does not disturb the nonreactive portion of the hydrodynamics. The interaction

of kinetics and hydrodynamics appears to be reasonably well, but certainly not exactly, reproduced by our numerical scheme.

II. THE COMPUTATIONAL METHOD

The hydrodynamic equations are presented and discussed in Appendix A. They were solved using the numerical difference technique described by Fromm[6]. The equation of state is described in Appendix B. The Fickett and Wood beta equation of state[7] form was chosen for the detonation products off the Chapman-Jouguet (C-J) isentrope. The pressure, volume, temperature, and energy values along the C-J isentrope were computed using the BKW codes[8]. The BKW codes use the Kistiakowsky-Wilson equation of state as modified by Cowan and Fickett[9]. The Grüneisen equation of state[10] was chosen for the undetonated explosive off the experimental Hugoniot. Pressures and volumes on the Hugoniot are available from experimental data, and Hugoniot temperatures were calculated using the technique of Walsh and Christian[10]. The equation of state for mixtures of condensed explosive and detonation products was computed assuming pressure and temperature equilibrium. The use of a first order reaction of the Arrhenius type described in Appendix A is apparently realistic. Zinn[11,12] has shown that the experimentally observed thermal initiation of explosives can be explained for the common explosives using Arrhenius first order reaction kinetics for adiabatic explosion times of hours down to 10 μsec or less. Our computed explosion times are in the 1-μsec range; thus the Arrhenius type kinetics is a reasonable choice.

The boundary conditions for the shock initiation calculations were chosen to approximate the experimental conditions that the plate ceases to push soon after initiation occurs at the plate-explosive interface; however, the essential features of the calculation are not changed if one permits the particle velocity

of the rear boundary to remain at its initial value throughout the calculation. The boundary conditions for the hot spot calculations were the usual ones for continuous systems.

The calculations were performed on an IBM 7090 electronic computer using the "SIN" code. A thousand mesh points could be used in the SIN code. Most of the computations in this report were performed with 500 mesh points. The graphs were prepared directly from computer output using a Stromberg-Carlson SC-4020 Microfilm Recorder.

III. RESULTS OF THE SHOCK INITIATION CALCULATIONS

The pressure-distance profiles for the shock initiation of nitromethane are shown in Figure 1. The shock travels into the explosive, causing shock heating and resultant chemical decomposition. Explosion occurs at the rear boundary, since it has been hot the longest. A detonation develops which has a C-J pressure and velocity characteristic of the explosive at the shock pressure and density. The detonation wave overtakes the shock wave and then decays to the normal density C-J pressure and velocity.

The computed and experimental data for the shock initiation of nitromethane, liquid TNT, and single-crystal PETN is shown in Table I.

The computed induction time (time to explosion) is primarily dependent upon the shock temperature. We probably know the shock temperature only to ±100°. In the case of nitromethane and PETN, we were lucky, and the computed shock temperatures were remarkably close to those required to reproduce the experimental induction times. However, we were not so lucky in the case of liquid TNT. The computed shock temperature was about 100° too high (1200 instead of 1100). We recomputed the shock temperatures using a heat capacity of 0.48 cal/g/°C instead of the literature value of 0.383 cal/g/°C, so as to obtain a shock temperature that would give the experimental induction time.

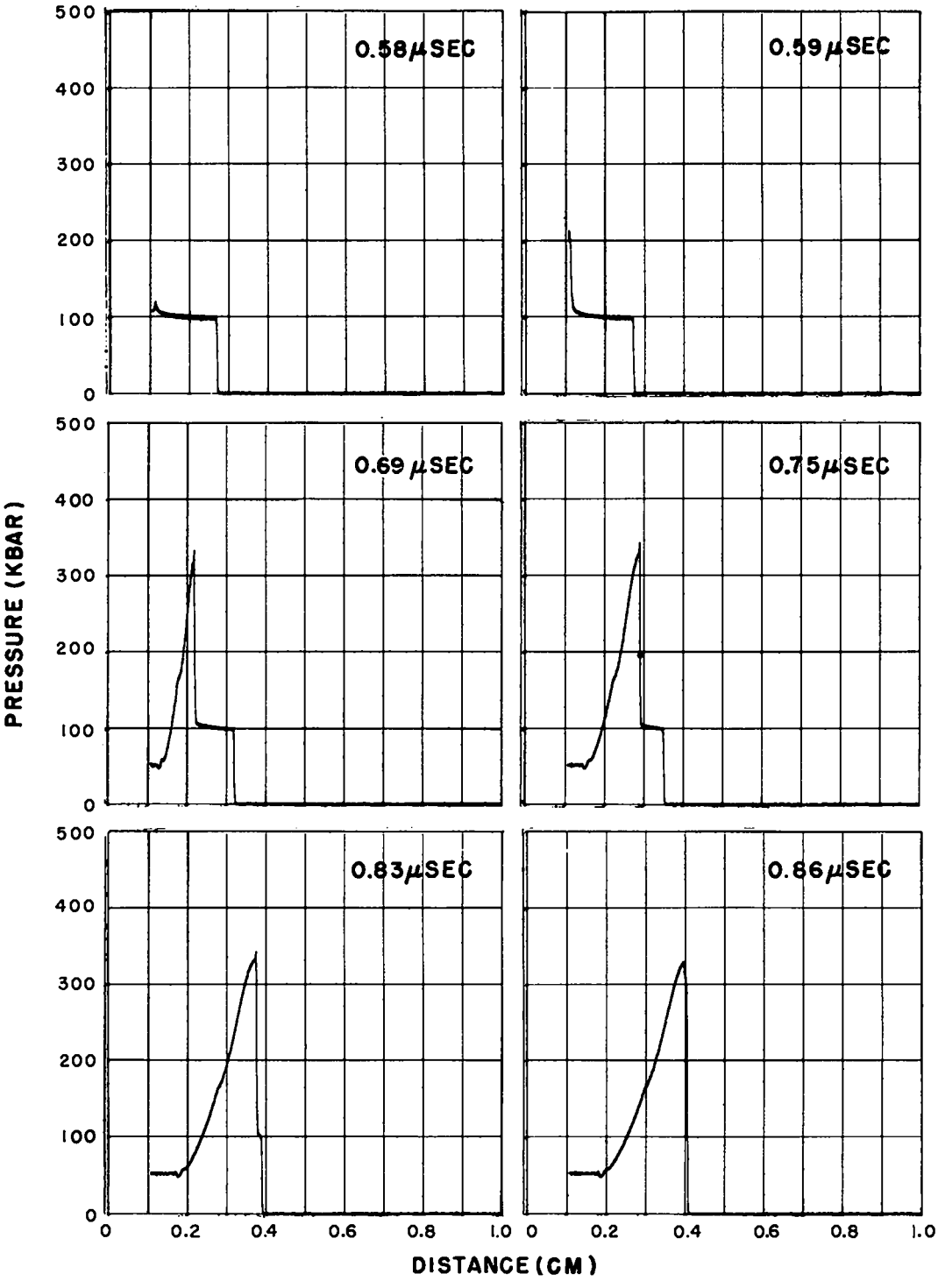

Fig. 1. Shock initiation of nitromethane by a 92 kbar shock.

Table I

SHOCK INITIATION OF NITROMETHANE, LIQUID TNT, AND PETN

Parameter	Input	Calculated	Experimental	BKW
		NITROMETHANE		
Particle Velocity (cm/μsec)	0.171		0.171 ± 0.01	
Initial Temperature (°K)	300		300	
Shock Pressure (mbar)		0.087	0.086 ± 0.005	
Shock Velocity (cm/μsec)		0.445	0.450	
Induction Time (μsec)		1.34	1.4 ± 0.7	
Det. Vel. + Part. Vel.* (cm/μsec)		1.044	1.022 ± 0.03	
Det. Vel. (Steady State)* (cm/μsec)		0.860	0.851 ± 0.02	0.847
Pressure* (mbar)		0.350	0.300	0.355
		LIQUID TNT		
Particle Velocity (cm/μsec)	0.176		0.176	
Initial Temperature (°K)	358.1		358.1	
Shock Pressure (mbar)		0.126	0.125	
Shock Velocity (cm/μsec)		0.490	0.490	
Induction Time** (μsec)		0.68	0.70	
Det. Vel. + Part. Vel.* (cm/μsec)		1.034	1.10 ± 0.1	
Det. Vel. (Steady State)* (cm/μsec)		0.858	0.925 ± 0.1	0.850
Pressure* (mbar)		0.460	--	0.466
		SINGLE-CRYSTAL PETN		
Particle Velocity (cm/μsec)	0.111		0.117	
Initial Temperature (°K)	298.17		298.17	
Shock Pressure (mbar)		0.115	0.112	
Shock Velocity (cm/μsec)		0.564	0.588	
Induction Time (μsec)		0.337	0.300	
Det. Vel. + Part. Vel.*** (cm/μsec)		0.985	1.090 ± 0.1	
Det. Vel. (Steady State)*** (cm/μsec)		0.870	0.973 ± 0.1	0.882
Pressure*** (mbar)		0.481	--	0.473

*In compressed explosive.

**C_V adjusted to give agreement between computed and experimental induction time.

***In compressed explosive, computed using small cell size.

The results of the computation of the shock initiation of PETN are of special interest. Our initial calculations were satisfactory until the shocked explosive detonated; then we obtained a flat-topped pressure profile with a very large detonation velocity. Because of the large reaction rate for PETN, the undetonated explosive next to the detonation front was shocked to a value well below the C-J volume when it completely decomposed. The pressure increased, and the velocity decreased, with decreasing mesh size until the C-J pressure and velocity was obtained. Thereafter the pressure and velocity did not change with further decrease in mesh size. It can be shown that decreasing Z (Arrhenius frequency factor) by a factor of 10 is approximately equivalent to decreasing ΔX and Δt by a factor of 10. Thus, we could keep the mesh size constant and decrease Z after the explosion started, or we could decrease the mesh size and keep Z constant. For the PETN calculation it is necessary to decrease the mesh size used in our calculations for nitromethane by a factor of 10^7. Satisfactory results may also be obtained by decreasing Z by 10^7 after the detonation has started, using the same mesh size as that used for nitromethane.

We conclude that the computed shock initiation of nitromethane, liquid TNT, and single-crystal PETN agrees qualitatively and quantitatively with the experimental data within experimental error.

IV. HYDRODYNAMIC HOT SPOT CALCULATIONS

The SIN code was used to investigate the propagation of hydrodynamic hot spots. The concept was first suggested by Francis Harlow of Group T-3.

Campbell, Davis, and Travis[1] have reported that "bubbles" about 0.7 mm in diameter cause hot spots in shocked nitromethane that will propagate, while bubbles about 0.4 mm in diameter cause hot spots that will not propagate. Evans, Harlow and Meixner[4] have investigated the interaction of a shock

wave with a bubble in nitromethane. The collapse of the bubble was accompanied by the generation of high temperatures in the liquid just above where the bubble had been. While calculational fluctuations precluded determination of the exact temperature profiles, the size of the hot region was of the same order of magnitude as the bubble. Increasing the bubble size results in increased hot spot size. Thus, a hot spot in shocked nitromethane may or may not propagate, depending primarily upon its size. When a hot spot has decomposed it sends a shock wave into the undetonated explosive and heats it. What occurs thereafter depends upon the initial strength of the shock wave and how well it is supported from the rear.

A. Temperature Hot Spots

The model for a temperature hot spot is a volume of uniform-density explosive containing a centered sphere of explosive at a higher energy than that of the surrounding medium. Thus, we have a hot spot of considerably higher temperature and only slightly higher pressure than the rest of the explosive.

Figure 2 shows the pressure-distance plots for a 0.292 cm radius hot spot in shocked nitromethane. Initially, at the boundary between the hot spot and the shocked nitromethane, a small shock is sent into the shocked nitromethane, and a rarefaction is sent back into the hot spot. At 0.03 μsec, part of the hot spot explodes and propagates through the remainder of the hot spot, which has been cooled by the rarefaction. A strong shock goes into the undetonated nitromethane, and a rarefaction goes back into the detonation products. The strongly shocked nitromethane at the hot spot boundary explodes at about 0.06 μsec, and the detonation propagates through the rest of the nitromethane. The hot spot propagates at a velocity of 0.856 cm/μsec, which is the computed equilibrium detonation velocity of the shocked nitromethane. The experimental detonation velocities of the Campbell, Davis,

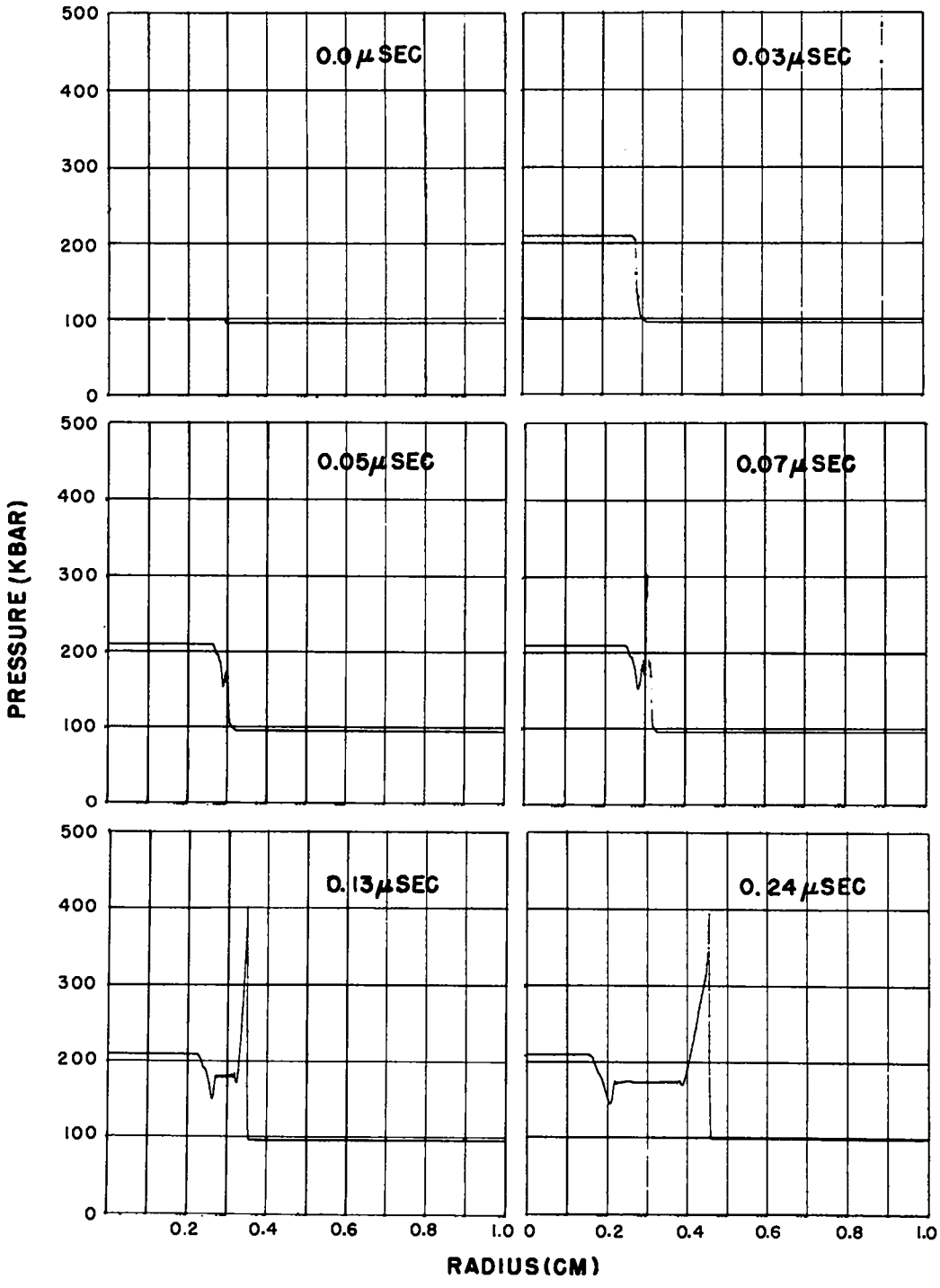

Fig. 2. Development of a detonation in shocked nitromethane (94.7 kbar, 1200°K) from a 0.292 cm radius spherical temperature hot spot (1404°K).

and Travis[1] hot spots in shocked nitromethane are 0.8 ± 0.1 cm/μsec.

Figure 3 shows in considerable detail the mechanism of propagation of a 0.06 cm radius hot spot. Initially, at the hot spot boundary, a small shock is sent into the shocked nitromethane, and a rarefaction is sent back into the hot spot. The pressure of the hot spot increases as a result of chemical reaction. At 0.0288 μsec, about 0.045 cm of the original hot spot explodes. At 0.035 μsec, the entire hot spot has exploded. A shock is sent into the undetonated explosive, and a rarefaction is sent into the detonation products. The undetonated explosive at the hot spot boundary does not explode until 0.08 μsec, or after an induction time of 0.045 μsec. In 0.1 μsec, the detonation is propagating at full velocity and pressure.

Figure 4 shows the pressure-distance profiles for a 0.0292 cm radius hot spot in shocked nitromethane. The behavior computed is essentially the same as for the larger hot spots except that the divergence of shock waves and the convergence of the rarefactions are sufficient to lower the strength of the shock at the hot spot interface so that propagation does not occur. The nitromethane at the boundary of the hot spot is cooling at 0.06 μsec, having a temperature of 1393°K, which is less than the initial hot spot temperature of 1404°K. At 0.08 μsec, the temperature of the boundary nitromethane has decreased to 1370°K.

Figure 5 shows the failure of a 0.27 cm radius hot spot in unshocked nitromethane. The pressure of a constant volume detonation in nitromethane initially at 1450°K is 81.5 kbar. A rarefaction travels into the detonation products, and a shock travels into the undetonated nitromethane. The shock temperature is sufficiently low that no reaction occurs, and the hot spot does not propagate. However, if an explosive has a constant volume detonation pressure that causes a shock in the undetonated explosive strong enough to give adequate shock heating, the hot spot propagates. An example is

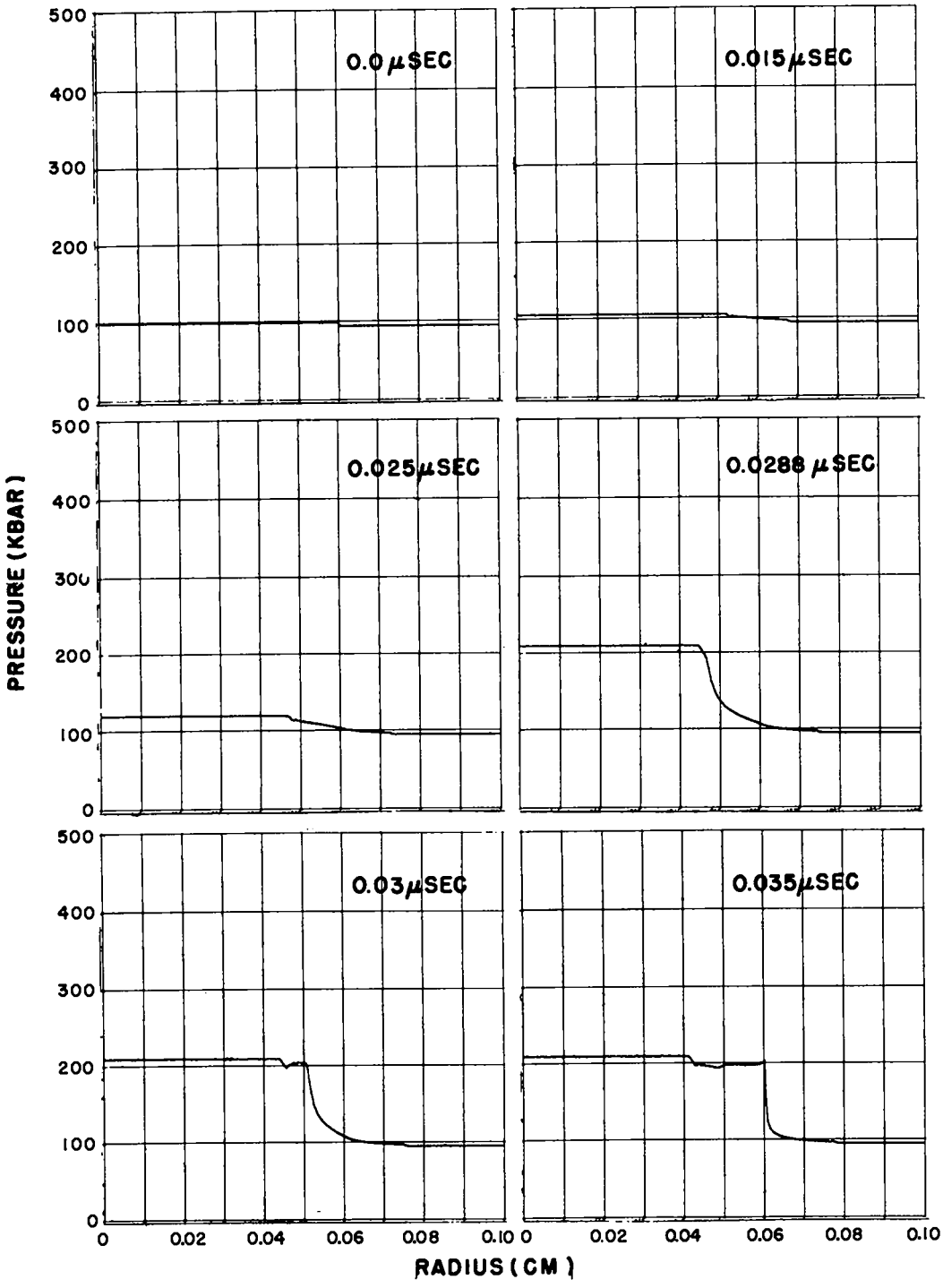

Fig. 3. Development of a detonation in shocked nitromethane (94.7 kbar, 1200°K) from a 0.06 cm radius spherical temperature hot spot (1404°K).

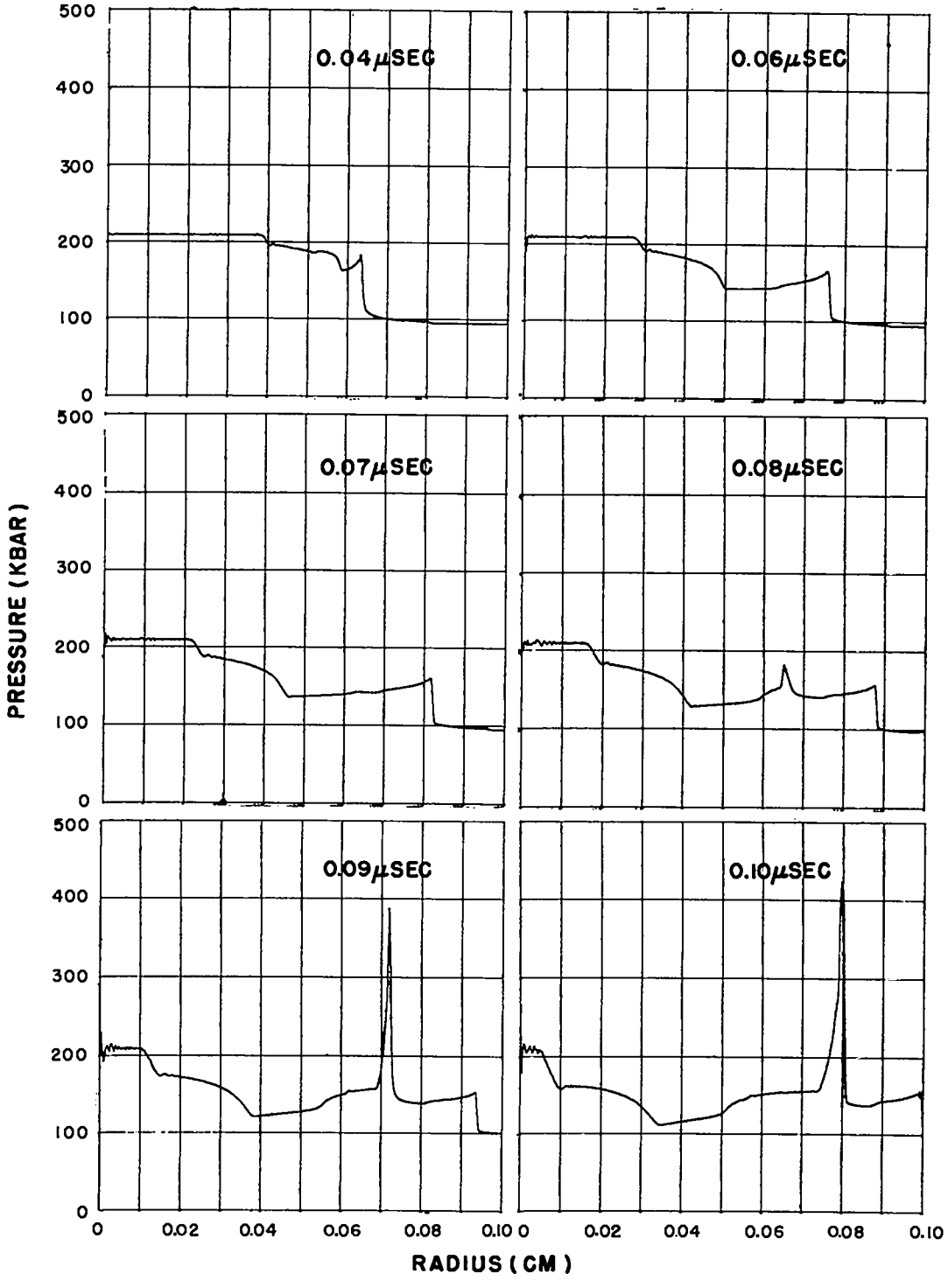

Fig. 3 Continued

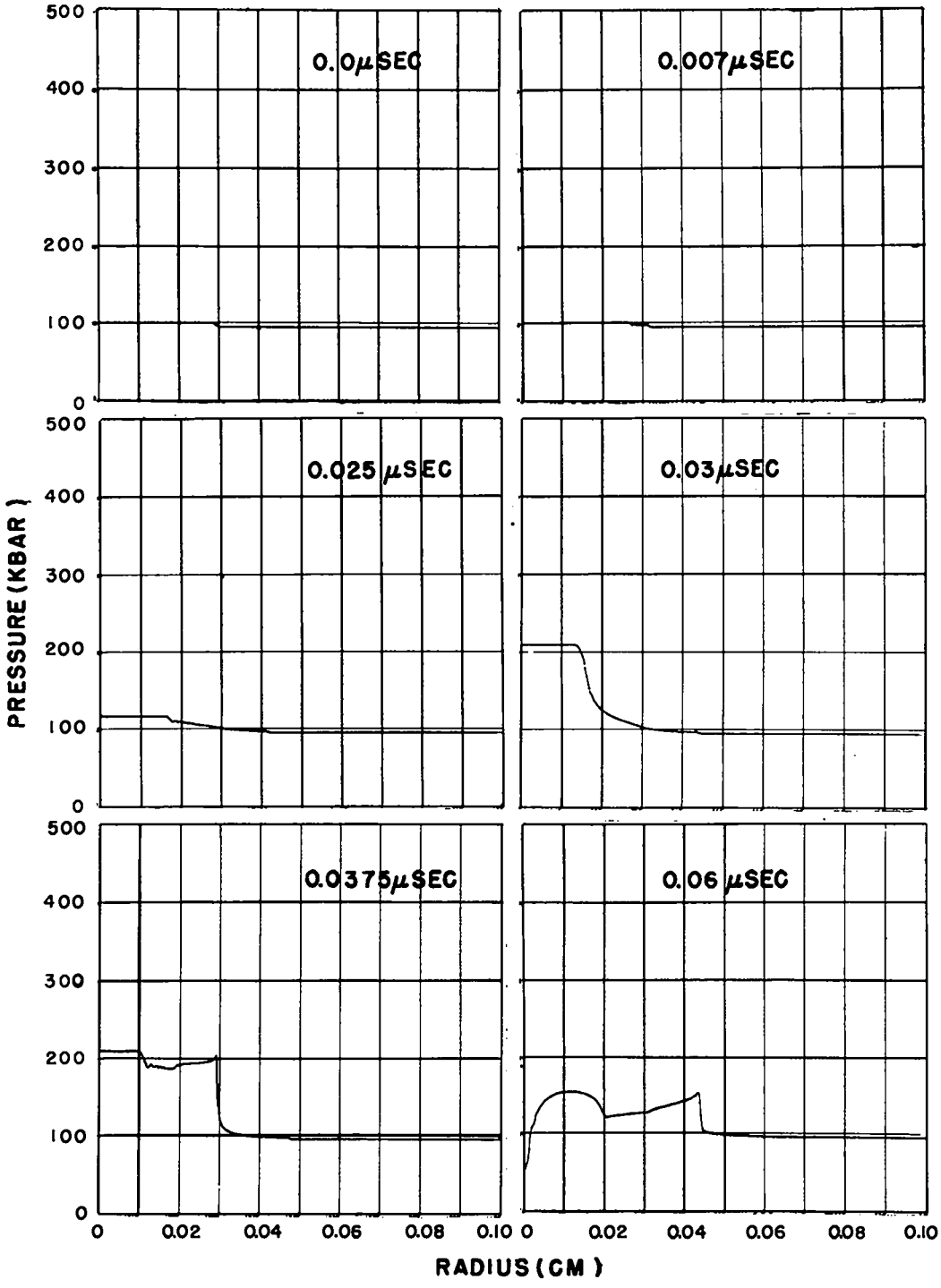

Fig. 4. Failure of a 0.0292 cm radius spherical temperature hot spot (1404°K) to develop into a detonation in shocked nitromethane (94.7 kbar, 1200°K).

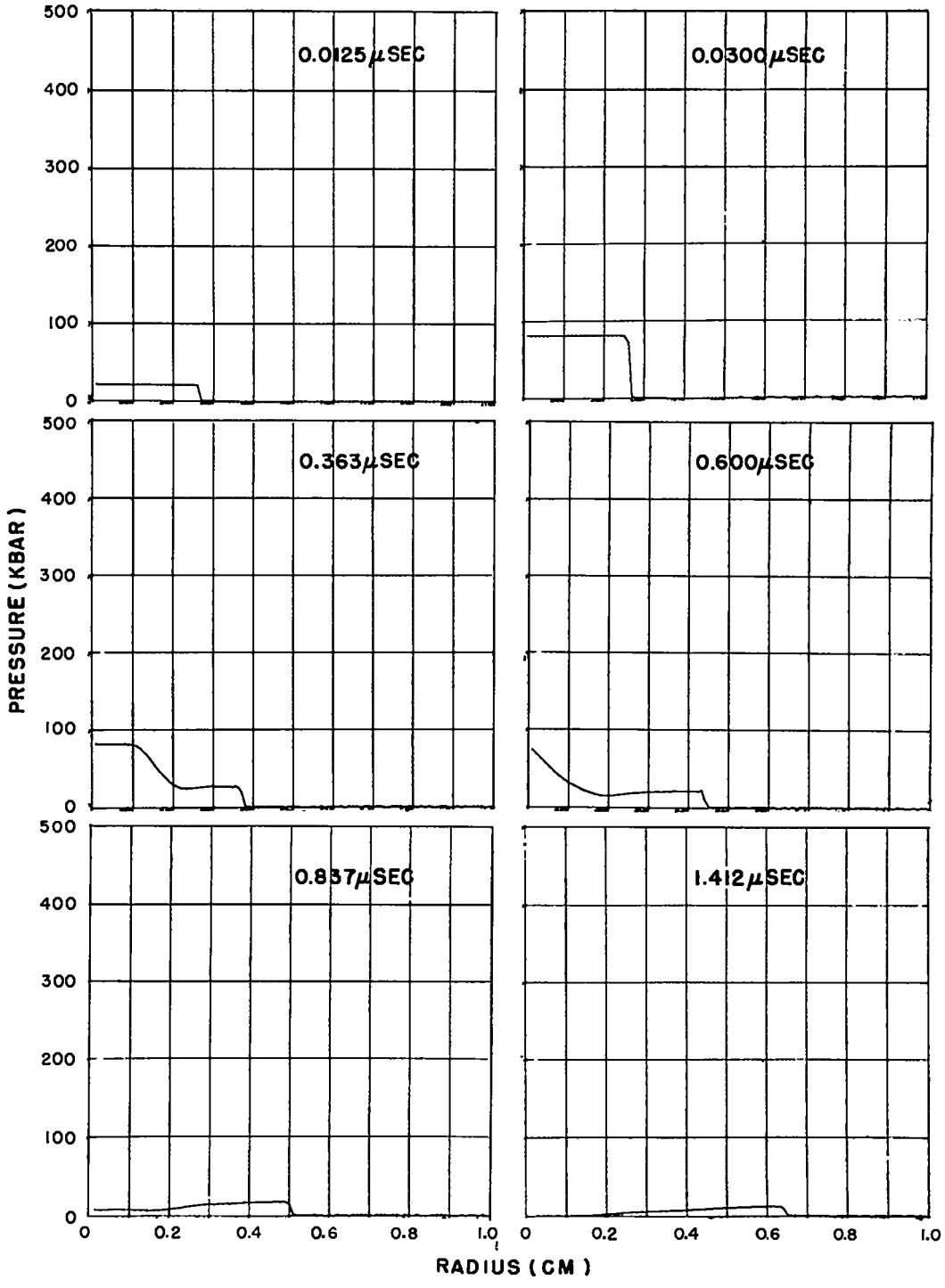

Fig. 5. Failure of 0.27 cm radius spherical temperature hot spot (1450°K) to develop into a detonation in unshocked nitromethane (300°K).

single-crystal PETN. The computed constant volume detonation pressure is 163 kbar for a PETN hot spot initially at 1500°K. A shock strong enough to propagate the detonation may be sent into the undetonated explosive.

Since we do not consider heat conduction in our calculations, it is of interest to determine if it might have any effect on our results for hot spots. Zinn[5] has shown that chemical reaction must be well under way by the end of the interval $t = 0.04\left(R^2\right)/k$, or heat conduction will prevent the hot spot from exploding. If we consider a hot spot with radius R of 0.06 cm, then t is 0.144 seconds. This is about 10^6 larger than the maximum times we are considering in our hot spot hydrodynamics.

The characteristics of temperature hot spots may now be described. Temperature hot spots of 0.06 cm radius and larger in shocked (90 kbar) nitromethane will propagate if the initial hot spot temperature is high enough that the hot spot explodes before the rarefaction arrives at its center. The hot spot might explode even after the rarefaction arrived at its center, since the rarefaction is weak.

Temperature hot spots of 0.03 cm radius and smaller in shocked (90 kbar) nitromethane will not propagate whether they explode or fail to explode before the rarefaction reaches their centers. The shock is not adequately supported from the rear.

As the pressure and temperature of the shocked nitromethane decrease, the critical size of the hot spots increases. The shock temperature in the undetonated explosive is less and, hence, must be maintained for a longer time if the boundary explosive is to explode. A larger hot spot is required to maintain the shock temperature for a longer time.

As the pressure and temperature of the shocked nitromethane increase, the critical size of the hot spot slowly decreases. The shock temperature in the undetonated explosive is higher and does not need to be maintained so

long for explosion to occur; however, the strong divergence of the shock wave and convergence of the rarefaction at the small diameters minimize the effect.

For nitromethane, a shock pressure and temperature exist below which any hot spot of reasonable size will not propagate by this mechanism. Large hot spots that explode in unshocked explosive may or may not propagate, depending upon the constant volume detonation pressure and the magnitude of the shock sent into the undetonated explosive.

B. Pressure Hot Spots

The model for a pressure hot spot is a centered sphere whose density and energy have been increased to a Hugoniot value larger than the density and energy of the surrounding explosive. This results in a hot spot of considerably higher pressure and temperature than the rest of the explosive.

Figure 6 shows the pressure-distance profiles for a 0.03 cm radius pressure (112 kbar, 1395°K) hot spot in shocked nitromethane (94.7 kbar, 1230°K). The rarefaction travels into the hot spot until, at 0.032 μsec, about 0.013 cm of the hot spot explodes. The rarefaction has cooled the hot spot sufficiently that it does not explode almost instantaneously, as it does in the case of the temperature hot spot. A shock is sent into the rest of the undecomposed hot spot, and at 0.034 μsec the shocked hot spot explosive decomposes and builds up to a C-J detonation pressure and velocity characteristic of the high density nitromethane. Upon arriving at the hot spot boundary, the shock pressure is so high that the detonation front continues unchanged.

Figure 7 shows the pressure-distance profiles for a 0.0175 cm radius pressure hot spot in shocked nitromethane. At 0.032 μsec, the first 0.0005 cm explodes; however, the converging rarefaction is sufficiently strong that the hot spot fails to propagate.

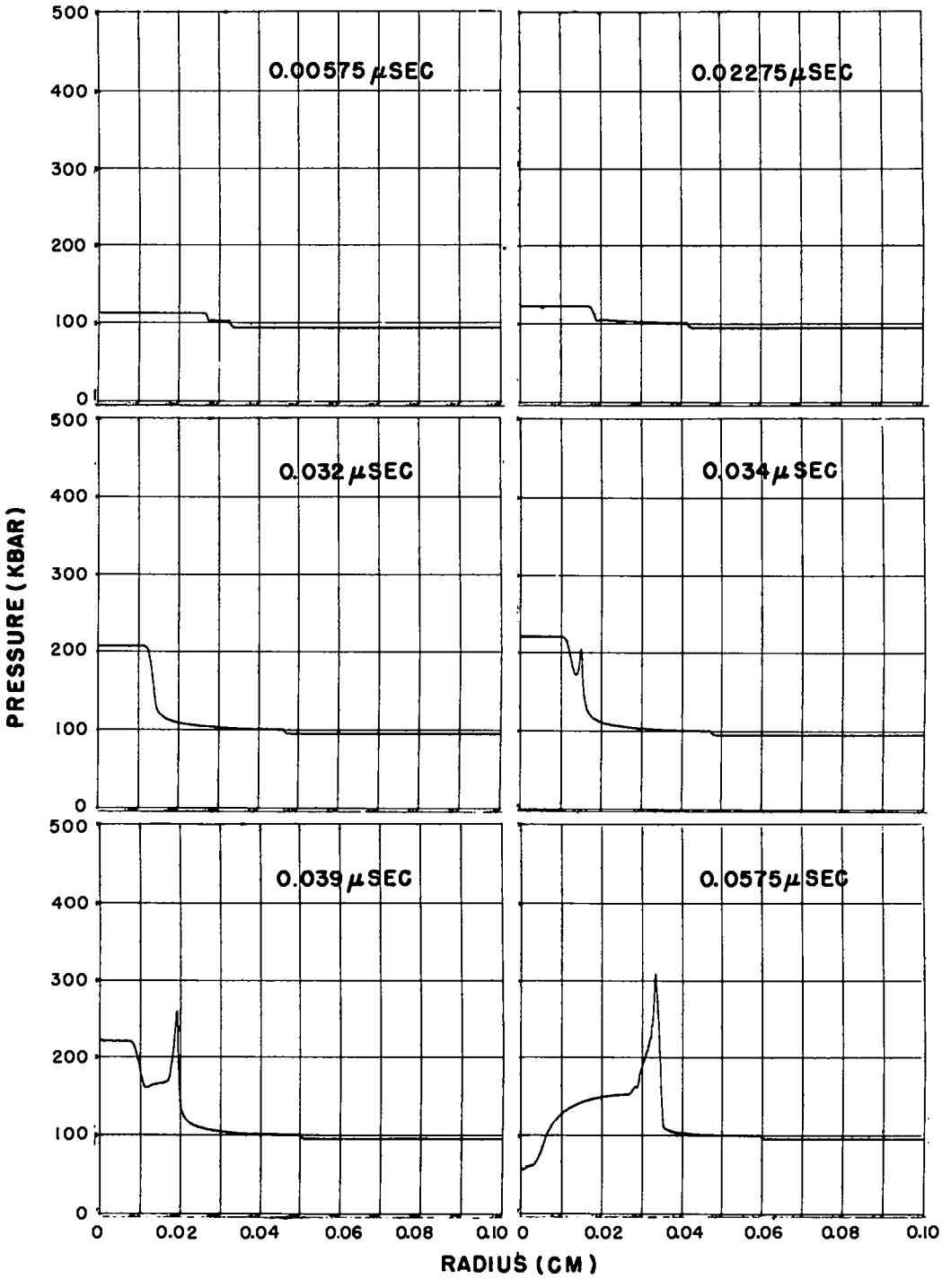

Fig. 6. Development of a detonation in shocked nitromethane (94.7 kbar, 1230°K) from a 0.03 cm radius spherical pressure hot spot (112 kbar, 1395°K).

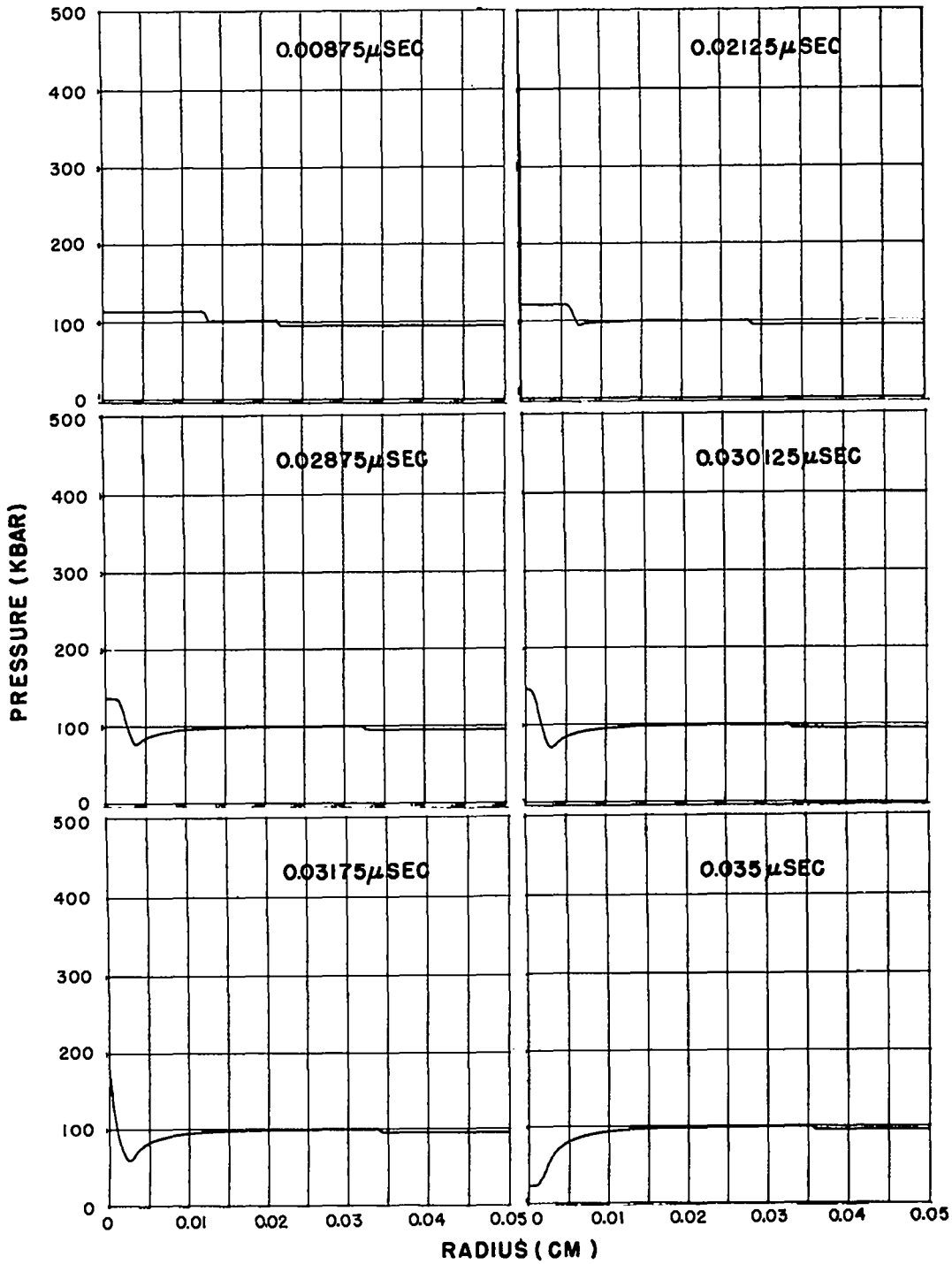

Fig. 7. Failure of a 0.0175 cm radius spherical pressure hot spot (112 kbar, 1395°K) to develop into a detonation in shocked nitromethane (94.7 kbar, 1230°K).

The characteristics of pressure hot spots may now be described. Pressure hot spots of 0.03 cm radius and larger in shocked (90 kbar) nitromethane will propagate if the initial hot spot temperature is high enough that the hot spot explodes before the rarefaction arrives near its center.

Pressure hot spots of 0.015 cm radius in shocked (90 kbar) nitromethane at temperatures of 1400°K and lower fail because the rarefaction arrives at the center of the hot spot before it explodes.

Pressure hot spots of about 0.0175 cm radius in shocked (90 kbar) nitromethane at 1400°K explode but fail to propagate because of the strong convergence of the rarefaction.

C. Hydrodynamic Hot Spot Summary

Over a considerable range of hot spot temperatures, the critical radius of a temperature hot spot in shocked (90 kbar) nitromethane is 0.03 to 0.06 cm. Over a considerable range of hot spot temperatures and pressures, the critical radius of a pressure hot spot is 0.015 to 0.03 cm. The computed critical radii of the hot spots are of the same order of magnitude as one expects from bubbles of 0.02 cm radius that were observed to form hot spots that fail, and bubbles of 0.035 cm radius that were observed to form hot spots that propagate. The hydrodynamic hot spot appears to be a satisfactory model for explaining the experimental observations.

V. CONCLUSIONS

The experimentally observed shock initiation of homogeneous explosives may be quantitatively reproduced using one-dimensional, numerical, reactive hydrodynamics, and realistic equations of state. A shock travels into the explosive, causing shock heating. Explosion occurs at the rear boundary, since chemical decomposition has been occurring there longest. A detonation develops and overtakes the shock wave.

The hydrodynamic hot spot is reasonably successful as a model for computing the critical sizes of hot spots in shocked nitromethane. Nitromethane hot spots of a size expected to result from interactions of a shock with the bubbles used experimentally may propagate or fail to propagate within the experimentally observed times of the order of 0.1 μsec. A hydrodynamic hot spot may fail to explode if the rarefaction reaches its center before it can explode adiabatically. If the hot spot explodes, it sends a shock wave into the undetonated explosive, which heats the explosive. Whether or not it propagates depends upon the initial strength of the shock wave and how well it is supported from the rear.

APPENDIX A

THE HYDRODYNAMIC EQUATIONS

The Lagrangian conservation equations in one dimension for slabs, cylinders, and spheres are:

$$\frac{dU}{dt} = -R^{\alpha-1}\frac{dP}{dM} \qquad \text{Conservation of momentum}$$

$$V = R^{\alpha-1}\frac{dR}{dM} \qquad \text{Conservation of mass}$$

$$\frac{dE}{dt} = -\frac{dPUR^{\alpha-1}}{dM} \qquad \text{Conservation of energy}$$

where $E = I + 0.5U^2$

$$\frac{dR}{dt} = U$$

$$dM = \rho_0 r^{\alpha-1}\,dr = \rho R^{\alpha-1}\,dR$$

where dM = element of mass per unit angle

The chemical reaction equation is

$$\frac{dW}{dt} = ZW\,e^{-E^*/R_gT}$$

The nomenclature is identical with that given at the end of this

Appendix, except that R is Eulerian distance, r is Lagrangian distance, and E is total energy. The treatment of total energy is further discussed in Appendix B.

The differencing of the differential equations was investigated using the Lax[13], Harlow and Daly[14], and Fromm[6] techniques.

The Lax scheme has an effective viscosity which varies inversely with the time increment. This scheme must be run with the largest time increment possible (the Courant Δt) to prevent serious diffusion. In any calculation involving both undetonated shocked explosive and its detonation products, the smaller time increment associated with the higher sound speed of the detonation products must be used in order to satisfy the Courant condition. The time increment is too small to give a reasonable effective viscosity for the undetonated shocked explosive. In addition, the calculation suffers from small oscillations, and in this region the two effects can result in a second explosion ahead of the main detonation wave. A solution to the problem can be obtained by using a differencing scheme in which the artificial viscosity is not a function of the time increment. Numerous such schemes are available; however, most of them suffer from fluctuations at the front of the shock wave which render them useless for systems in which the reaction rates have an exponential dependence on temperature. This problem was studied by Zovko[15] and Enig[3], and they chose the Lax scheme to avoid the fluctuations. They, however, were not attempting the fine resolution described here and therefore did not observe the other difficulties associated with the Lax scheme.

We investigated two attractive difference schemes using the artificial viscosity method to determine if we could dampen the fluctuations and still retain the desirable characteristics.

The first method investigated was the cell-centered method of Harlow and Daly[14]. In this method the parameters are cell-centered, the energy is

conserved locally, entropy is changed only by the viscosity, and the system is accurate and stable to infinitesimal fluctuations. However, it was not possible to dampen the fluctuations sufficiently using any of the usual forms for the artificial viscosity[16].

The second difference scheme we investigated was that described by Fromm[6]. The Richtmyer-von Neumann type of viscosity did not sufficiently damp the small fluctuations associated with the Fromm difference equation. The Landshoff type of viscosity[16] required careful adjustment of the arbitrary constant, but at best was still not successful. However, the particle in cell (PIC) type of viscosity[16] was successful in damping the fluctuations.

In the Fromm type of difference equations, the pressure, temperature, energy, and specific volume of the cells are considered to be located at the centers of mass of the elements, and the particle velocity is considered to be located at the boundary between the cells.

The energy is conserved locally in the Fromm type of difference equations. This may be shown by summing the total energy in Equation (6) over all the mesh points, resulting in

$$\sum_{j=1}^{j=N} \left[E_j^{n+1} - E_j^n \right]$$

where $E = \left(I + 0.5U^2\right)M$. All the terms of the sum cancel except at the end points. Thus, the difference of the total energy of the space at two consecutive times is just the flux at the two boundaries.

In the Fromm type of difference equations, one finds internal consistency for the case of slabs. For example, from Equations (4) and (5), one may derive the difference form of the conservation equation $dV/dt = dU/dM$.

One can show, by approximating the parameters as Taylor expansions, that the Fromm difference equations formally approach the differential equations as the time increment and cell mass decrease.

Using the Fromm difference equations, one can show, by substituting the difference equations into the thermodynamic equation TdS = dI + PdV, that entropy is not conserved in the absence of viscosity.

Fromm[6] has shown that the difference equations are conditionally stable to infinitesimal fluctuations, using the von Neumann method, in which the perturbation is expanded in a Fourier series and a given Fourier component is examined.

Thus, the difference equations are sufficiently accurate and stable to infinitesimal fluctuations, and energy is conserved locally. The equations can be shown not to conserve entropy in the absence of viscosity. Numerically we have shown that the difference equations with the PIC viscosity are conditionally stable.

I. THE SIN DIFFERENCE EQUATIONS FOR SLABS, CYLINDERS, OR SPHERES

A. Initial Conditions

$$R_{j+\frac{1}{2}} = J\Delta R \tag{1}$$

where $j = 0, 1, 2, \ldots$

$$R_{-\frac{1}{2}} = U_{\text{piston}}(\Delta t)$$

$$M_j = \rho_0 \left(R_{j+\frac{1}{2}}\right)^{\alpha-1} \Delta R \tag{2}$$

B. Conservation Equations

$$U_{j+\frac{1}{2}}^{n+\frac{1}{2}} = U_{j+\frac{1}{2}}^{n-\frac{1}{2}} + \frac{(\Delta t)\left(R_{j+\frac{1}{2}}^{n}\right)^{\alpha-1}}{0.5\left(M_j + M_{j+1}\right)} \left[\left(P_j^n - P_{j+1}^n\right) + \left(q_j^n - q_{j+1}^n\right)\right] \tag{3}$$

$$R_{j+\frac{1}{2}}^{n+1} = R_{j+\frac{1}{2}}^{n} + U_{j+\frac{1}{2}}^{n+\frac{1}{2}} (\Delta t) \tag{4}$$

$$V_j^{n+1} = \left(R_{j+\frac{1}{2}}^{n+1}\right)^{\alpha-1} \frac{\left(R_{j+\frac{1}{2}}^{n+1} - R_{j-\frac{1}{2}}^{n+1}\right)}{M_j} \tag{5}$$

$$I_j^{n+1} = I_j^n + \frac{(\Delta t)}{M_j} \left\{ \left[\frac{M_j P_{j-1}^n + M_{j-1} P_j^n}{M_j + M_{j-1}} + 0.5\left(q_j^n + q_{j-1}^n\right) \right] U_{j-\frac{1}{2}}^{n+\frac{1}{2}} \left(R_{j-\frac{1}{2}}^{n+1}\right)^{\alpha-1} \right.$$

$$\left. - \left[\frac{M_{j+1} P_j^n + M_j P_{j+1}^n}{M_j + M_{j+1}} + 0.5\left(q_j^n + q_{j+1}^n\right) \right] U_{j+\frac{1}{2}}^{n+\frac{1}{2}} \left(R_{j+\frac{1}{2}}^{n+1}\right)^{\alpha-1} \right\}$$

$$+ \frac{1}{8} \left[\left(U_{j+\frac{1}{2}}^{n-\frac{1}{2}} + U_{j-\frac{1}{2}}^{n-\frac{1}{2}}\right)^2 - \left(U_{j+\frac{1}{2}}^{n+\frac{1}{2}} + U_{j-\frac{1}{2}}^{n+\frac{1}{2}}\right)^2 \right] \tag{6}$$

C. Chemical Reaction Equation

$$W_j^{n+1} = W_j^n - \Delta t Z W_j^n \, e^{-E^*/R_g T_j^n} \tag{7}$$

where $1 \geq W \geq 0$

D. Equation of State

P_j^{n+1}, T_j^{n+1}, and C_j^{n+1} are computed using the HOM equation of state subroutine from V_j^{n+1}, I_j^{n+1} and W_j^{n+1}.

E. Artificial Viscosity

$$q_j^{n+1} = \frac{K}{V_j^{n+1}} (0.5) \left(U_{j-\frac{1}{2}}^{n+\frac{1}{2}} + U_{j+\frac{1}{2}}^{n+\frac{1}{2}}\right) \left(U_{j-\frac{1}{2}}^{n+\frac{1}{2}} - U_{j+\frac{1}{2}}^{n+\frac{1}{2}}\right) \tag{8}$$

if $\left(U^{n+\frac{1}{2}}_{j-\frac{1}{2}} - U^{n+\frac{1}{2}}_{j+\frac{1}{2}}\right)$ is positive, otherwise $q^{n+1}_j = 0$.

F. Time Increment

One may use a constant Δt or compute it for each cycle.

$$\Delta t = (CK)\Delta R \frac{V^{n+1}_j}{V_0 C^{n+1}_j} \tag{9}$$

G. Boundary Conditions for Shock Sensitivity Calculations

$U^n_{-\frac{1}{2}}$ and $U^{n+1}_{-\frac{1}{2}} = U_{piston}$ where boundary is at j = 0

if $W^n_{j+\frac{1}{2}} > 0.5$, otherwise = 0

$$q^n_{-1} = q^n_1$$

$$P^n_{-1} = P^n_1$$

$R_{-\frac{1}{2}}$ is computed using Equation (4)

II. NOMENCLATURE

α = 1 for slabs, 2 for cylinders, and 3 for spheres

C = sound speed in cm/μsec

CK = constant of about 0.1

Δt = time in μsec

E* = activation energy

I = internal energy in mbar-cc/g

j = net point of Lagrangian net

K = constant of about 2

M = mass

n = time cycle

P = pressure in mbar

q = artificial viscosity

R = radius in cm

R_g = gas constant

ρ_0 = initial density in g/cc

T = temperature in °K

U = particle velocity in cm/μsec

V = volume in cc/g

$V_0 = 1/\rho_0$

W = mass fraction of the undecomposed explosive

Z = frequency factor

APPENDIX B

THE EQUATION OF STATE

Initially we investigated the equation of state used by Enig[3]. He used the Tait equation for the undetonated explosive and the gamma-law equation of state for the detonation products. We adjusted the parameters in the Tait equation of state to give pressures and volumes in reasonable agreement with the experimental Hugoniot values over the range of interest. The parameters were also adjusted to give temperatures that agreed with the values computed using the Walsh and Christian technique[10].

The growth of detonation from an initiating shock was computed using the Tait and gamma-law equation of state for nitromethane, liquid TNT, and PETN. The computed detonation velocities in the compressed explosive were less than those experimentally observed. The major cause of this discrepancy is that the detonation velocity is not a function of density with a gamma-law equation of state, but is only a function of energy. Likewise, the C-J temperatures and pressures were in marked disagreement with the observed values.

Thus, a more realistic equation of state was necessary if we were to reproduce the experimental results. The one we used is called the HOM equation of state.

The Fickett and Wood[7] beta equation of state was chosen as the form

for the detonation products. The pressure, volume, temperature, and energy values along the C-J isentrope were computed using the BKW codes[8] which use the Kistiakowsky-Wilson equation of state as modified by Cowan and Fickett[9].

The Grüneisen equation of state[10] was chosen for the undetonated explosive. Hugoniot pressures and volumes are available from experimental data. Temperatures on the Hugoniots were calculated using the technique of Walsh and Christian[10].

The equation of state for mixtures of condensed explosive and detonation products is derived in Equations (1) through (19) of this Appendix. The equations require a single iteration for each problem, hence the equation of state for mixtures requires considerable computer time.

The equation of state and rate parameters are shown in Table BI. The fits to the detonation products isentrope are good from 1 to 5×10^{-4} mbar. The heat capacity of the detonation products was computed using the BKW C-J parameters (shown in Table BII) for the shocked explosive; Equations (7) through (11) to compute $E - E_i$ and T_i; and Equation (12) to compute C'_V. The Hugoniot data used for liquid TNT were reported by Garn[17]. The Hugoniots used for nitromethane and single-crystal PETN were approximated by W. Davis from available experimental data. The fits to the Hugoniot pressures and temperatures are good from 1 to 350 kbar. We used the activation energy and frequency factors of Cook and Taylor[18] for PETN; of Cottrell[19] for nitromethane; and of Zinn[12] for liquid TNT.

I. THE CONDENSED EXPLOSIVE AND DETONATION PRODUCT EQUATION OF STATE

Knowing E, V, and W, we calculate P, T, C.

Table BI

EQUATION OF STATE AND RATE PARAMETERS

Parameter	Nitromethane		Liquid TNT		PETN	
Detonation Product		Exp		Exp		Exp
A	-3.0177389	00	-3.5356454	00	-3.4346496	00
B	-2.4028066	00	-2.4873789	00	-2.4498765	00
C	+1.9981153	-01	+2.7864444	-01	+2.1221113	-01
D	+9.9666715	-03	+5.3344652	-02	+6.0697867	-03
E	-4.4261494	-03	-2.7491409	-02	-5.7596766	-03
K	-1.5762640	00	-1.7153682	00	-1.5954648	00
L	+5.3780073	-01	+5.7252810	-01	+4.8780484	-01
M	+1.2202885	-02	+4.6863081	-02	+4.6779526	-02
N	-2.6100200	-03	+1.0161346	-03	+9.1462157	-04
O	-2.9775278	-04	-7.8496783	-05	-7.5662542	-05
Q	+7.7365662	00	+7.6317317	00	+7.4428658	00
R	-5.2925794	-01	-4.7735596	-01	-5.2085389	-01
S	+9.2967764	-02	+1.1398787	-01	+1.0458042	-01
T	+1.2878571	-02	+2.6182746	-02	+1.4337016	-02
U	-5.9641444	-03	-1.5211680	-02	-1.1391835	-02
C_V'	+5.5600000	-01	+5.0000000	-01	+4.6700000	-01
Z	+6.0000000	-02	+6.0000000	-02	+1.0000000	-01
Condensed Explosive						
A_s	-8.6335924	00	-5.6489393	01	-9.8284779	00
B_s	-1.6490344	01	-2.8785482	02	+3.4325262	01
C_s	-1.5367448	01	-5.9739302	02	+1.3815194	02
D_s	-1.1037889	01	-5.5607584	02	+1.3998427	02
E_s	-4.2114837	00	-1.9124016	02	+4.5106916	01
F_s	+6.0426166	00	-1.0712113	00	-1.3504381	02
G_s	+4.4825758	00	-4.8502353	01	-8.0905992	02
H_s	+1.4829189	01	-1.2282460	02	-1.7206747	03
I_s	+7.6203073	00	-1.3376445	02	-1.5994725	03
J_s	-2.4398587	-02	-5.0515048	01	-5.4551108	02
γ_s	+6.8050000	-01	+1.6600000	00	+7.7000000	-01
C_V	+4.1400000	-01	+4.8000000	-01	+2.6000000	-01
V_0	+8.8652000	-01	+6.9444000	-01	+5.6497000	-01
Chemical Reaction						
E*	+5.3600000	04	+4.1100000	04	+5.2300000	04
Z	+4.0000000	08	+1.7100000	07	+1.2600000	17

Table BII

BKW COMPUTED C-J PARAMETERS

Explosive	Density (g/cc)	E_0 (kcal/mole)	P_{C-J} (mbar)	Det. Vel. (cm/μsec)	T_{C-J} (°K)	V_{C-J} (cc/mole)	γ
Nitromethane	1.128	-14.92	0.151	0.687	2960	15.33	2.53
(shocked to 81 kbar)	1.762	3.91	0.355	0.847	2810	10.83	2.56
Liquid TNT	1.447	3.41	0.173	0.675	2960	15.54	2.81
(shocked to 125 kbar)	2.261	87.76	0.466	0.850	2860	10.68	2.50
PETN	1.770	-95.5	0.330	0.832	2890	12.59	2.72
(shocked to 112 kbar)	2.210	-47.89	0.473	0.882	2610	10.95	2.63

A. Condensed Explosive $\left(W = 1, \text{ then } E = E_s, V = V_s\right)$

Hugoniot pressures and volumes are known experimentally, Hugoniot temperatures are computed using the Walsh and Christian technique[10]. The Hugoniot data is fitted by the method of least squares to Equations (1) and (2).

$$\ln P_H = A_s + B_s \ln V_s + C_s\left(\ln V_s\right)^2 + D_s\left(\ln V_s\right)^3 + E_s\left(\ln V_s\right)^4 \tag{1}$$

$$\ln T_H = F_s + G_s \ln V_s + H_s\left(\ln V_s\right)^2 + I_s\left(\ln V_s\right)^3 + J_s\left(\ln V_s\right)^4 \tag{2}$$

$$E_H = \frac{1}{2} P_H\left(V_0 - V_s\right) \tag{3}$$

$$P_s = \frac{\gamma_s}{V_s}\left(E_s - E_H\right) + P_H \tag{4}$$

where $\gamma_s = V\left(\frac{\partial P}{\partial E}\right)_V$

$$T_s = T_H + \frac{\left(E_s - E_H\right)(23{,}899)}{C_V} \tag{5}$$

$$C_s = \sqrt{-PV_s\left[B_s + 2C_s \ln V_s + 3D_s\left(\ln V_s\right)^2 + 4E_s\left(\ln V_s\right)^3\right]} \tag{6}$$

(assumes that the slope of the Hugoniot curve is approximately the same as the slope of the adiabat at the same V_s)

B. Detonation Products $\left(W = 0, \text{ then } E = E_g, V = V_g\right)$

The pressure, volume, temperature, and energy values of the detonation products along the C-J isentrope are computed using the Kistiakowsky-Wilson equation of state[8] and fitted by the method of least squares to Equations (7) through (9).

$$\ln P_i = A + B\ln V_g + C\left(\ln V_g\right)^2 + D\left(\ln V_g\right)^3 + E\left(\ln V_g\right)^4 \tag{7}$$

$$\ln E_i' = K + L\ln P_i + M\left(\ln P_i\right)^2 + N\left(\ln P_i\right)^3 + O\left(\ln P_i\right)^4 \tag{8}$$

$$E_i = E_i' - Z$$

where Z is a constant used to change the standard state to make it consistent with the condensed explosive standard state

$$\ln T_i = Q + R\ln V_g + S\left(\ln V_g\right)^2 + T\left(\ln V_g\right)^3 + U\left(\ln V_g\right)^4 \tag{9}$$

$$-\frac{1}{\beta} = R + 2S\ln V_g + 3T\left(\ln V_g\right)^2 + 4U\left(\ln V_g\right)^3 \tag{10}$$

$$P_g = \left(\frac{1}{\beta V_i}\right)\left(E_g - E_i\right) + P_i \tag{11}$$

where $\beta = \frac{1}{V}\left(\frac{\partial E}{\partial P}\right)_V$

$$T_g = T_i + \frac{\left(E_g - E_i\right)(23{,}899)}{C_V'} \tag{12}$$

$$C_g = \sqrt{-PV_g\left[B + 2C\ln V_g + 3D\left(\ln V_g\right)^2 + 4E\left(\ln V_g\right)^3\right]} \tag{13}$$

(assumes that the slope of the adiabat at P_i, V_g is the same as at P, V_g).

C. Mixture of Condensed Explosive and Detonation Products

$$V = WV_s + (1 - W)V_g \tag{14}$$

$$E = WE_s + (1 - W)E_g \tag{15}$$

$$P = P_g = P_s \tag{16}$$

$$T = T_g = T_s \tag{17}$$

One may derive an expression for V_g or V_s as a function of E, V, and W by multiplying Equation (5) by $\left(W/C'_V\right)$ and Equation (12) by $\left[(1 - W)/C_V\right]$ and adding the resulting equations. Substituting T for T_g and T_s, per Equation (17), and E for $\left[WE_s + (1 - W)E_g\right]$, per Equation (15), one obtains

$$T = \frac{23{,}899}{C_V W + C'_V(1 - W)} \left\{ E - \left[WE_H - E_i(1 - W)\right] + \frac{1}{23{,}899}\left[T_H C_V W + T_i C'_V(1 - W)\right]\right\} \tag{18}$$

Equating Equations (4) and (11), one obtains an equation into which Equation (18) may be substituted to obtain

$$P_H - P_i + \left(\frac{\gamma_s C_V}{V_s} - \frac{C'_V}{\beta V_g}\right)\left(\frac{1}{C_V W + C'_V(1 - W)}\left\{E - \left[WE_H + E_i(1 - W)\right] + \frac{1}{23{,}899}\left[T_H C_V W + T_i C'_V(1 - W)\right]\right\}\right) - \frac{1}{23{,}899}\left(\frac{\gamma_s C_V T_H}{V_s} - \frac{C'_V T_i}{\beta V_g}\right) = 0 \tag{19}$$

With Equation (14), we now have an expression for V_g or V_s as a function of the known parameters E, V, and W. In the HOM code, if W was between 0.999 and 0.7, we iterated on V_s, and if W was less than 0.7, we iterated on V_g. Knowing V_g and V_s, one may compute the other unknowns. The largest sound speed was assumed to be that of the mixture.

II. NOMENCLATURE

C = sound speed in cm/μsec

C_V = heat capacity of condensed explosive in cal/g/°C

C'_V = heat capacity of detonation products in cal/g/°C

E = total internal energy in mbar-cc/g

P = pressure in mbar

T = temperature in °K

V = total volume in cc/g

V_0 = initial volume of condensed explosive in cc/g

W = mass fraction of undecomposed explosive

Subscripts

g = detonation products

H = Hugoniot

i = isentrope

s = condensed explosive

LITERATURE CITED

1. Campbell, A. W., Davis, W. C., and Travis, J. R., "Shock Initiation of Detonation in Liquid Explosives", Phys. of Fluids, 4, 498 (1961).

2. Hubbard, Harmon W., and Johnson, M. H., "Initiation of Detonations", J. Appl. Phys., 30, 765 (1959).

3. Enig, Julius W., "Growth of Detonation from an Initating Shock", Third Symposium on Detonation, ONR symposium report ACR-52, 534 (1960).

4. Evans, Martha E., Harlow, Francis H., and Meixner, Billy D., "Interaction of Shock or Rarefaction with a Bubble", Phys. of Fluids, 5, 651 (1962).

5. Zinn, John, "Initiation of Explosions by Hot Spots", J. Chem. Phys., 36, 1949 (1962).

6. Fromm, Jacob E., "Lagrangian Difference Approximations for Fluid Dynamics", Los Alamos Scientific Laboratory Report LA-2535 (1961).

7. Fickett, W., and Wood, W. W., "A Detonation-Product Equation of State Obtained from Hydrodynamic Data", Phys. of Fluids, 1, 528 (1958).

8. Mader, Charles L., "Detonation Performance Calculations Using the Kistiakowsky-Wilson Equation of State", Los Alamos Scientific Laboratory Report LA-2613 (1961).

9. Cowan, R. D., and Fickett, W., "Calculation of the Detonation Properties of Solid Explosives with the Kistiakowsky-Wilson Equation of State", J. Chem. Phys., 24, 932 (1956).

10. Walsh, John M., and Christian, Russell H., "Equation of State of Metals from Shock Wave Measurements", Phys. Rev., 97, 1544 (1955).

11. Zinn, John, and Mader, Charles L., "Thermal Initiation of Explosives", J. Appl. Phys., 31, 323 (1960).

12. Zinn, John, and Rogers, R., "Thermal Initiation of Explosives" (to be published).

13. Lax, Peter D., "Weak Solutions of Nonlinear Hyperbolic Equations and their Numerical Computation", Communs. Pure Appl. Math., 7, 159 (1954).

14. Harlow, Francis H., and Daly, Bart, Los Alamos Scientific Laboratory, private communication.

15. Zovko, C. T., and Macek, A., "A Computational Treatment of the Transition from Deflagration to Detonation in Solids", Third Symposium on Detonation, ONR symposium report ACR-52, 606 (1960).

16. Longley, H. J., "Methods of Differencing in Eulerian Hydrodynamics", Los Alamos Scientific Laboratory Report LAMS-2379 (1959).

17. Garn, W. B., "Determination of the Unreacted Hugoniot for Liquid TNT", J. Chem. Phys., 30, 819 (1959).

18. Cook, M. A., and Taylor, M., "Isothermal Decomposition of Explosives", Ind. Eng. Chem., 48, 1090 (1956).

19. Cottrell, T. L., Graham, T. E., and Reid, T. Y., "The Thermal Decomposition of Nitromethane", Trans. Faraday Soc., 47, 584 (1951).